AAS 05-158

A Direct Method for Fuel Optimal Maneuvers of Distributed Spacecraft in Multiple Flight Regimes

Steven P. Hughes[1]

D. S. Cooley[2]

Jose J. Guzman[3]

We present a method to solve the impulsive minimum fuel maneuver problem for a distributed set of spacecraft. We develop the method assuming a non-linear dynamics model and parameterize the problem to allow the method to be applicable to multiple flight regimes including low-Earth orbits, highly-elliptic orbits (HEO), Lagrange point orbits, and interplanetary trajectories. Furthermore, the approach is not limited by the inter-spacecraft separation distances and is applicable to both small formations as well as large constellations. Semianalytical derivatives are derived for the changes in the total ΔV with respect to changes in the independent variables. We also apply a set of constraints to ensure that the fuel expenditure is equalized over the spacecraft in formation. We conclude with several examples and present optimal maneuver sequences for both a HEO and libration point formation.

Introduction

In this paper, we present a direct approach to solve the impulsive, minimum fuel maneuver problem for a distributed set of spacecraft. To equalize the fuel expenditure among spacecraft, we enforce a set of nonlinear constraints. We present an explanation of the method and the mathematical theory assuming a general, nonlinear dynamics model that can be expressed in an inertial or rotating coordinate system depending on the problem being solved. This ensures the method is applicable to a wide range of spaceflight regimes. Furthermore, since a nonlinear dynamics model is used, the method is not limited to small

[1]Aerospace Engineer, Flight Dynamics Analysis Branch, NASA Goddard Space Flight Center, (301) 286-0145, (301) 286-0369 (FAX), email: Steven.P.Hughes@nasa.gov

[2]Aerospace Engineer, Flight Dynamics Analysis Branch, NASA Goddard Space Flight Center, (301) 286-6653, (301) 286-0369 (FAX), email: D.S.Cooley@nasa.gov

[3]Aerospace Engineer, a.i. solutions, current address: Applied Physics Lab, Mail Stop MP3 W-135 11100 Johns Hopkins Rd. Laurel, MD 20723-6099

inter-spacecraft separations and is equally applicable to large constellations and close formations.

Trajectory optimization has a rich history and many techniques have been developed over the last fifty years. Most techniques can be classified as either direct or indirect. Betts[1] presents an excellent survey of trajectory optimization techniques. Guzman[2] *et.al.* present a survey of indirect methods. The approach developed here is a direct method and is an extension of techniques that have their origins in research performed during the Apollo era[3,4] and later extended by D'Amario[5] *et. al.*, and Howell[6,7] *et. al.* Their are several new contributions contained in this work. First, the method is generalized to permit minimum fuel optimization for a maneuver sequence involving a set of m spacecraft. We have also generalized the method to find the optimal launch vehicle injection orbit to minimize fuel during the initial spacecraft deployment phase. Finally, we have reformulated the cost function to remove a naturally occurring singularity in the gradient, without loss of generality.

We begin this paper with a mathematical problem statement defining the cost and constraint functions. The cost function is the sum of the total ΔV of all spacecraft over an entire maneuver sequence. The parameterization of the problem is discussed for two types of maneuver sequences: initialization and reconfiguration. Next, we discuss how to evaluate the cost and constraints. The approach requires solving a number of Initial Value Problems (IVP) and Two Point Boundary Value Problems (TPBVP). However, given the speed of modern computers, the method is surprisingly fast. Next, the gradient of the cost function and the Jacobian of the constraints are derived. We discuss numerical issues in implementing this approach. We conclude the paper with several test problems in different flight regimes to demonstrate the applicability of the method. A brief explanation of the notation is included in Appendix 3.

Problem Statement and Parameterization

There are numerous ways to pose the minimum fuel formation maneuver problem. We assume that the desired relative motion is driven by mission requirements and has been determined a-priori. The goal is to develop a technique to achieve the desired relative motion in a minimum fuel manner. We define the minimum fuel problem for a formation of m spacecraft, where the trajectory of the k^{th} spacecraft has n_k total maneuvers, as

Given: $\mathbf{r}_{o_k}$, $\mathbf{v}_{o_k}$, t_{o_k},$\mathbf{r}_{f_k}$, $\mathbf{v}_{f_k}$, t_{f_k}

where $\mathbf{r}_{o_k}$, $\mathbf{v}_{o_k}$, and t_{o_k} are the initial position, velocity, and epoch of the k^{th} spacecraft respectively. $\mathbf{r}_{f_k}$ and $\mathbf{v}_{f_k}$ are the final position and velocity respectively of the k^{th} spacecraft at a reference epoch t_{f_k}

Solve:

$$\min(J) \tag{1}$$

where

$$J = \sum_{k=1}^{m} \Delta V_k \tag{2}$$

where m is the number of spacecraft and ΔV_k is the total weighted ΔV expended by the k^{th} spacecraft and is calculated using

$$\Delta V_k = \sum_{j=1}^{n_k} f_s(\Delta v_{jk}) \Delta v_{jk} \tag{3}$$

where Δv_{jk} is the j^{th} maneuver on the k^{th} trajectory. The scalar function $f_s(\Delta v_{jk})$ in Eq. (3) is included to remove a singularity in the derivative of J for small Δv_{jk}. This function will be discussed in detail in a later section. For now it suffices to say that $f_s(\Delta v_{jk}) = 1$ for values of Δv_{jk} large enough not to cause numerical problems. When appropriate, we impose the following set of constraints to equalize the ΔV among the spacecraft.

$$\begin{aligned}
(\Delta V_1 - \Delta V_2)^2 &\leq tol_1 && (4)\\
(\Delta V_2 - \Delta V_3)^2 &\leq tol_2 && (5)\\
&\vdots \\
(\Delta V_{m-1} - \Delta V_m)^2 &\leq tol_{m-1} && (6)\\
(\Delta V_1 - \Delta V_m)^2 &\leq tol_m && (7)
\end{aligned}$$

where tol_1 is the desired tolerance for constraint one and so on.

We assume a dynamics model given by the second order differential equation

$$\ddot{\mathbf{r}} = \mathbf{f}(\mathbf{r}, \dot{\mathbf{r}}, t) \tag{8}$$

The formulation of the cost and constraints, and their derivatives, is performed for the general nonlinear dynamics model seen in Eq. (8). We discuss the specific dynamics model used for software implementation and validation in a later section.

At the heart of solving an optimization problem is the problem parameterization. In general, the cost function J shown in Eq. (2) is a scalar function of vectors that we can write as

$$J = \sum_{k=1}^{m} \Delta V_k = J(\mathbf{X}, \mathbf{C}) \tag{9}$$

where $\mathbf{X}$ is the vector of independent variables being manipulated by an optimization routine, and $\mathbf{C}$ is a vector of constants associated with the problem. The constraints in Eqs. (4) - (7) can be written as

$$\mathbf{G} = \text{diag}\left(\mathbf{Z}\Delta\mathbf{V}\Delta\mathbf{V}^T\mathbf{Z}^T\right) = \mathbf{G}(\mathbf{X}, \mathbf{C}) \leq \mathbf{TOL} \tag{10}$$

where $\mathbf{\Delta V} = [\Delta V_1 \;\; \Delta V_2 \;\; \ldots \;\; \Delta V_{m-1} \;\; \Delta V_m]^T$, $\mathbf{Z}$ is constant matrix discussed in a later section, and $\mathbf{TOL}$ is a vector of tolerances associated with the constraints. Before attempting to solve the problem we must choose which variables and degrees of freedom associated with the problem are to be included in $\mathbf{X}$, which will be varied by a numerical optimization routine, and which degrees of freedom are to be included in $\mathbf{C}$ and treated as constants. The choice of $\mathbf{X}$ and $\mathbf{C}$ will influence the convergence properties of the numerical routine and determine the types of problems the method can solve.

In the remainder of this section, we discuss two parameterizations to solve the impulsive minimum fuel maneuver problem for distributed spacecraft. For convenience, we categorize the types of maneuver sequences as initialization sequences or maintenance/reconfiguration sequences. In an initialization sequence, all spacecraft begin at a common time and location on the same orbit. An initialization sequence is performed to take each member spacecraft from the common parking orbit to its desired final location defined by a final orbit and time. In a maintenance maneuver sequence, the spacecraft are not initially located on the same orbit and hence are not collocated before the maneuvers are performed. The fuel optimal maintenance sequence is a more general problem and we begin by discussing the approach taken here.

Maintenance and Reconfiguration Sequence

An illustration of a formation reconfiguration sequence is shown in Figure 1. For simplicity the diagram only illustrates a two-spacecraft sequence. Before the beginning of the maneuver sequence, each spacecraft is located on a unique orbit. We define the initial orbit for the k^{th} spacecraft, $\mathcal{P}_{ok}$, as the locus of points that are the solutions to the initial value problem

$$\mathbf{r}_{1k} = \phi^r(t_{1k}, t_{ok}, [\mathbf{r}_{ok}, \mathbf{v}_{ok}]) \tag{11}$$

for varying values of t_{1k}, the time at which the k^{th} spacecraft performs its first maneuver. Recall that $\mathbf{r}_{ok}$ and $\mathbf{v}_{ok}$ are the position and velocity respectively, of the k^{th} spacecraft at some reference epoch t_{ok}. Throughout the paper we use ϕ^r to denote the position portion of the solution to the Initial Value Problem (IVP) of the differential equation shown in Eq. (8). The initial conditions to the IVP shown in Eq. (11) are contained in square brackets. The initial time is the second argument and the final time is the first argument.

The goal of the reconfiguration sequence is to depart from the trajectories defined by $\mathcal{P}_{ok}$, and move each spacecraft to a new location on $\mathcal{P}_{fk}$ which is defined as the locus of points that are the solution to the initial value problem

$$\mathbf{r}_{n_k k} = \phi^r(t_{n_k k}, t_{fk}, [\mathbf{r}_{fk}, \mathbf{v}_{fk}]) \tag{12}$$

for varying values of $t_{n_k k}$, where n_k is the number of maneuvers on the k^{th} trajectory, and $\mathbf{r}_{fk}$ and $\mathbf{v}_{fk}$ are the desired final position and velocity respectively, of the k^{th} spacecraft at some reference final epoch t_{fk}. According to this definition, $t_{n_k k}$ is the time of the last maneuver of the k^{th} spacecraft.

Between the initial and final maneuvers, the k^{th} spacecraft can perform intermediate maneuvers at locations $\mathbf{r}_{jk}$ given by

$$\mathbf{r}_{jk} \quad \begin{cases} 2 \leq & j & \leq n_k - 1 \\ 1 \leq & k & \leq m \end{cases} \tag{13}$$

Note that the reason $2 \leq j \leq n_k - 1$ is because $\mathbf{r}_{1k}$ and $\mathbf{r}_{n_k k}$ are determined from the initial value problems shown in Eq. (11) and (12). Because we allow the time of the first and last maneuver for each spacecraft to vary, as well as the times of the interior maneuvers, we see that t_{ik}, the maneuver times, are given by

$$t_{ik} \quad \begin{cases} 1 \leq & i & \leq n_k \\ 1 \leq & k & \leq m \end{cases} \tag{14}$$

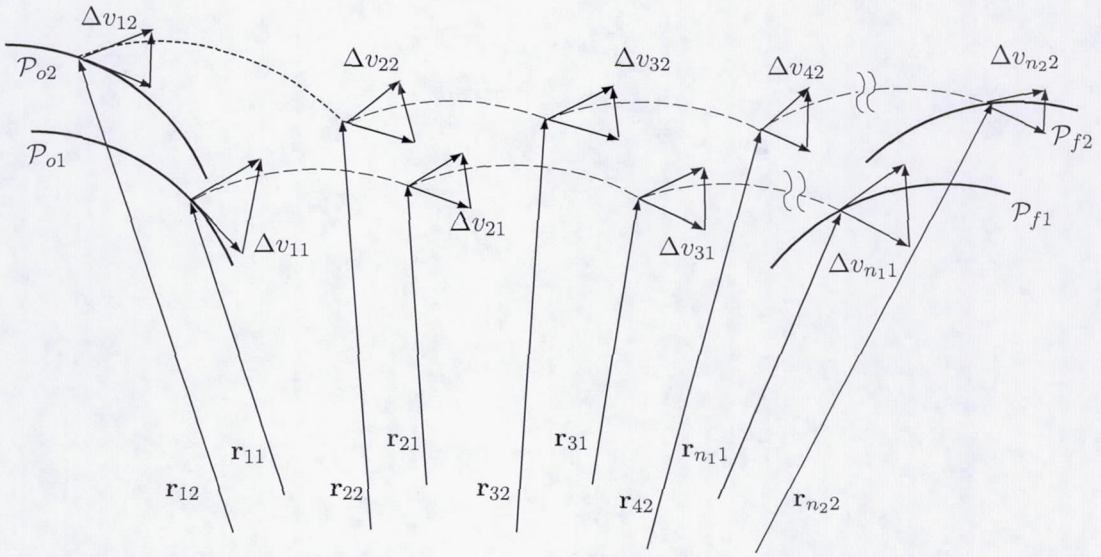

Figure 1 Formation Maintenance and Reconfiguration Illustration

There may be numerical difficulties if t_{ik} is not ordered such that $t_{2k} > t_{1k}$. This is discussed in a later section.

From Eqs. (11-14) we see that the variables that define the maneuver sequence are: t_{1k}, t_{ok}, $\mathbf{r}_{ok}$, $\mathbf{v}_{ok}$, t_{fk}, $\mathbf{r}_{fk}$, $\mathbf{v}_{fk}$, $\mathbf{r}_{jk}$, and t_{ik}. We can now parameterize the problem by choosing which variables to include in $\mathbf{X}$ and which to include in $\mathbf{C}$. For the general minimum fuel reconfiguration problem we choose to include as independent variables the time of the first maneuver of the k^{th} spacecraft, t_{1k}, the times of the interior maneuvers, t_{ik}, and the times of the final maneuvers, $t_{n_k k}$. We also include the locations of the interior maneuvers, $\mathbf{r}_{jk}$, as independent variables. We treat the state components t_{ok}, $\mathbf{r}_{ok}$, and $\mathbf{v}_{ok}$ that define the initial orbit, and the state components t_{fk}, $\mathbf{r}_{fk}$, and $\mathbf{v}_{fk}$ that define the final orbits, as constants. In summary, for the maintenance and reconfiguration problem we can write

$$\mathbf{X} = \left[t_{ik} \ \mathbf{r}_{jk}^T \right]^T \quad \begin{cases} 2 \leq & j & \leq n_k - 1 \\ 1 \leq & i & \leq n_k \\ 1 \leq & k & \leq m \end{cases} \tag{15}$$

$$\mathbf{C} = \left[\ t_{ok} \ \mathbf{r}_{ok}^T \ \mathbf{v}_{ok}^T \ t_{fk} \ \mathbf{r}_{fk}^T \ \mathbf{v}_{fk}^T \ \right]^T \tag{16}$$

The parameterization of the reconfiguration problem shown in Eqs. (15) and (16) is chosen such that the boundary conditions at $\mathbf{r}_{1k}$ and $\mathbf{r}_{n_k k}$ are satisfied implicitly. The optimizer is not tasked with satisfying another set of complicated non-linear constraints to satisfy the boundary conditions along the initial and final orbits $\mathcal{P}_{ok}$ and $\mathcal{P}_{fk}$ respectively. The down-side to this approach is that for each cost function evaluation we must solve a number of initial value problems (IVP) and two point boundary value problems (TPBVP). Solution of the TPBVPs is discussed in a later section. In the next section we discuss the parameterization of the initialization sequence.

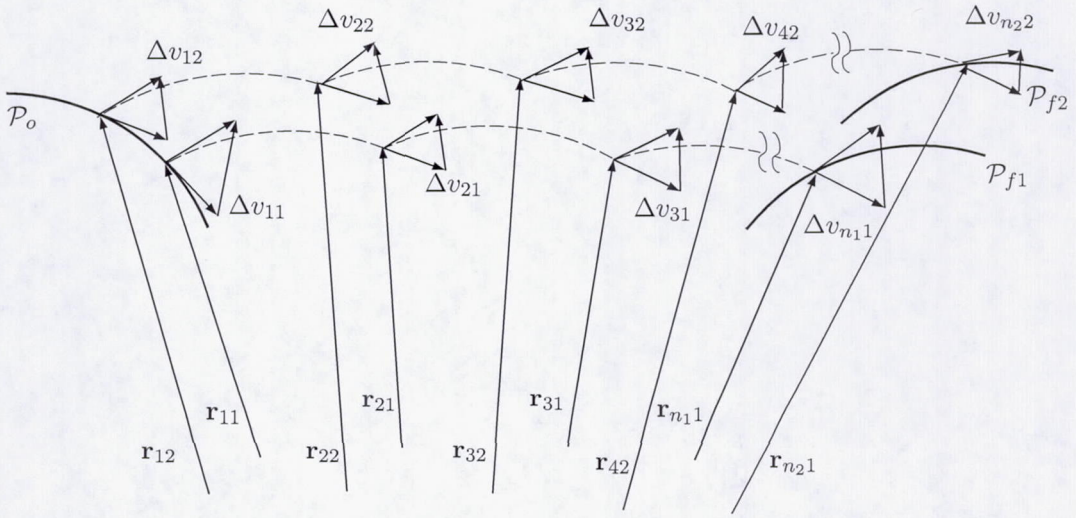

Figure 2 Formation Initialization Illustration

Initialization Sequence

The second type of maneuver sequence we address is an initialization sequence. In an initialization sequence, all spacecraft initially lie on a common orbit defined by the locus of points $\mathcal{P}_o$, as shown in Figure 2. Hence, for the initialization sequence we have

$$\mathbf{r}_{ok} = \mathbf{r}_o \ , \quad \mathbf{v}_{ok} = \mathbf{v}_o \ , \quad t_{ok} = t_o \quad \text{and} \ , \quad \mathcal{P}_{ok} = \mathcal{P}_o \tag{17}$$

We refer to $\mathcal{P}_o$ as the injection orbit and it may or may not be known a-priori. For large formations that may require significant fuel expenditure from all spacecraft in formation to achieve the desired relative geometry, it may be desirable to include the injection orbit itself as an independent variable. In this case, the solution to the optimization problem yields the minimum fuel initialization trajectory for each spacecraft as well as the optimal launch vehicle injection orbit. Referring to Figure 2, we see that although all spacecraft initially lie on $\mathcal{P}_o$, it is not required that all spacecraft perform their first maneuver in the initialization sequence at the same epoch and hence the spacecraft can depart from $\mathcal{P}_o$ at different locations. The location of the first maneuver for the k^{th} spacecraft is determined by the epoch of its first maneuver t_{1k}, and the state vector that defines $\mathcal{P}_o$. We assume that $\mathcal{P}_o$ is unique trajectory defined by the locus of points that is the solution to the following IVP for varying values of t_{1k}:

$$\mathbf{r}_{1k} = \phi^r(t_{1k}, t_o, [\mathbf{r}_o, \mathbf{v}_o]) \tag{18}$$

where t_o, $\mathbf{r}_o$, and $\mathbf{v}_o$, are the launch vehicle injection conditions, and t_{1k} is the time of the first maneuver of the k^{th} spacecraft. There is a unique final trajectory for the k^{th} spacecraft defined by the locus of points, $\mathcal{P}_{fk}$, which is the solution to the following IVP for varying values of $t_{n_k k}$:

$$\mathbf{r}_{n_k k} = \phi^r(t_{n_k k}, t_{fk}, [\mathbf{r}_{fk}, \mathbf{v}_{fk}]) \tag{19}$$

We assume the values t_{fk}, $\mathbf{r}_{fk}$, and $\mathbf{v}_{fk}$ have been determined a-priori to maximize the mission return. Hence these values are constants for the initialization problem.

For complete generality, we assume that the epoch of the initial maneuver for each spacecraft and the epoch of the final maneuver to insert the spacecraft into its location in formation can freely vary. Note that the initial epoch of the first maneuver of the k^{th} spacecraft, t_{1k} is not the same as t_o. The epoch t_o is part of the state vector that uniquely determines the injection orbit, while t_{1k} is the epoch when the k^{th} spacecraft departs from the injection orbit. We also assume that the times and locations of the interior maneuvers for all spacecraft can freely vary. For the initialization problem we define $\mathbf{X}$ and $\mathbf{C}$ as follows:

$$\mathbf{X} = \left[\; t_o \; \mathbf{r}_o^T \; \mathbf{v}_o^T \; t_{ik} \;\; \mathbf{r}_{jk}^T \; \right]^T \qquad \begin{cases} 2 \leq & j & \leq n_k - 1 \\ 1 \leq & i & \leq n_k \\ 1 \leq & k & \leq m \end{cases} \tag{20}$$

$$\mathbf{C} = \left[\; t_{fk} \; \mathbf{r}_{fk}^T \; \mathbf{v}_{fk}^T \; \right]^T \tag{21}$$

The parameterization of the cost and constraint functions in an optimization problem greatly influence the convergence properties of the method. In this section, we discussed a parameterization of the minimum fuel maneuver problem for two types of maneuver sequences for a set of distributed spacecraft. Given the problem parameterizations developed in this section, we are ready to look into the details of evaluating the cost and constraint functions.

Cost and Constraint Function Evaluation

In this section we take the problem parameterization given by $\mathbf{X}$ and $\mathbf{C}$ in the last section and discuss how to calculate the cost $J(\mathbf{X}, \mathbf{C})$ and the constraints $\mathbf{G}(\mathbf{X}, \mathbf{C})$. Calculating the cost and constraints is similar for both the initialization and the reconfiguration problem and so we address them simultaneously. The first step is to redimensionalize the vector of independent variables $\mathbf{X}$. Once we have a dimensionalized set of variables given by $\mathbf{X}$ and $\mathbf{C}$, we solve a set of IVPs to obtain the position vectors that define the locations of the first and last maneuvers of each spacecraft. The next step is to solve a set of TPBVPs that yield Δv_{jk}. Finally, we solve for the cost and constraints using Eqs. (2), (3) and (32). Each step is discussed in more detail below.

Step 1: Redimensionalize X

It is often necessary to work with nondimensional variables when solving optimization problems using numerical methods. We begin by assuming that the numerical optimization process uses non-dimensional variables where the transformation from dimensional to nondimensional variables is given by

$$\mathbf{X}' = \text{diag}(\mathbf{X}_f)^{-1}\mathbf{X} - \mathbf{X}_s \tag{22}$$

where $\mathbf{X}'$ is the nondimensional form of $\mathbf{X}$, $\text{diag}(\mathbf{X}_f)$ is a matrix with $\mathbf{X}_f$ on the diagonal and zeros for the off-diagonal terms, and $\mathbf{X}_f$ and $\mathbf{X}_s$ are vectors of the same length as $\mathbf{X}$. We assume that $\text{diag}(\mathbf{X}_f)^{-1}$ exists. The inverse transformation is simply

$$\mathbf{X} = \text{diag}(\mathbf{X}_f)(\mathbf{X}' + \mathbf{X}_s) \tag{23}$$

It is more convenient to work in dimensional variables to evaluate the cost and constraints and the redimensionalization is performed before step 2 is performed. $\mathbf{X}_f$ and $\mathbf{X}_s$ are chosen according to the numerical issues associated with the particular problem being solved.

Step 2: Solve IVPs

To evaluate the cost and constraints, we need to be able to calculate

$$\Delta v_{jk} = \|\mathbf{v}_{jk}^{+} - \mathbf{v}_{jk}^{-}\| \quad \begin{cases} 1 \leq j \leq n_k \\ 1 \leq k \leq m \end{cases} \tag{24}$$

where a superscript "-" denotes a condition immediately before an impulse maneuver, and a superscript "+" denotes a condition immediately after an impulsive maneuver. The quantities $\mathbf{v}_{1k}^{-}$ and $\mathbf{v}_{n_k k}^{+}$ are determined by solving the following initial value problems

$$\mathbf{v}_{1k}^{-} = \phi^{v}(t_{1k}, t_{ok}, [\mathbf{r}_{ok}, \mathbf{v}_{ok}]) \tag{25}$$

$$\mathbf{v}_{n_k k}^{+} = \phi^{v}(t_{n_k k}, t_{fk}, [\mathbf{r}_{fk}, \mathbf{v}_{fk}]) \tag{26}$$

where ϕ^{v} denotes the velocity portion of the solution to the IVP, and t_{fk}, $\mathbf{r}_{fk}$, and $\mathbf{v}_{fk}$ are contained in $\mathbf{C}$ and treated as constants. If we are solving a maintenance problem, t_{ok}, $\mathbf{r}_{ok}$, and $\mathbf{v}_{ok}$ are also contained in $\mathbf{C}$. However, if we are solving an initialization problem then the initial boundary conditions may be contained in $\mathbf{X}$. To solve the TPBVPs found in the next step we will need $\mathbf{r}_{1k}$ and $\mathbf{r}_{n_k k}$. However, these are simply the position portions of the solution to the IVPs in Eq. (25) and (26).

Step 3: Solve TPBVPs

The remaining components of the impulsive maneuver vectors needed to calculate Eqs. (24) are determined by solving a set of TPBVPs. From Step 2 we found $\mathbf{r}_{1k}$ and $\mathbf{r}_{n_k k}$, and the variables $\mathbf{r}_{ik}$ and t_{jk} are contained in $\mathbf{X}$. Therefore, we know the positions and times for all maneuvers and we have N Lambert's problems to solve where N is given by

$$N = \sum_{k=1}^{m} (n_k - 1) \tag{27}$$

There are numerous well-known approaches to solving Lambert's problem. We use a simple multiple shooting method outlined below. The algorithm is described as follows where we drop the subscript k, for now, to simplify the notation. Given an initial position $\mathbf{r}_j$ and an initial velocity $\mathbf{v}_j$, both at time t_j, find $\delta\mathbf{v}_j$ applied at time t_j so that we achieve $\mathbf{r}_{j+1}$ at t_{j+1}. Figure 3 illustrates the problem. The dark black arc denotes the path a spacecraft would follow if no $\delta\mathbf{v}_j$ were applied. For this arc, the final position denoted by $\mathbf{r}_a$ is not equal to the desired final position $\mathbf{r}_{j+1}$. Hence, for the dark black are, $\delta\mathbf{r}_{j+1} \neq 0$. The dashed arc denotes the trajectory that is the solution to Lambert's problem. For this arc $\mathbf{r}_{j+1} = \mathbf{r}_a$, or $\delta\mathbf{r}_{j+1} = 0$. To solve for $\delta\mathbf{v}_j$ such that $\delta\mathbf{r}_{j+1} = 0$ first define $\mathbf{x}_j$ as

$$\mathbf{x}_j = \begin{bmatrix} \mathbf{r}_j \\ \mathbf{v}_j \end{bmatrix} \tag{28}$$

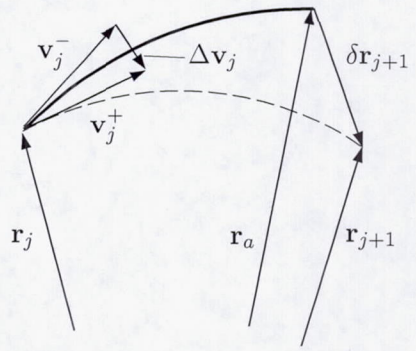

Figure 3 Illustration of One Trajectory Arc

then $\delta\mathbf{x}_{j+1}$ is given by

$$\delta\mathbf{x}_{j+1} = \mathbf{\Phi}\left(t_{j+1}, t_j\right)\delta\mathbf{x}_j \tag{29}$$

where t_{j+1} and t_j are fixed. We can write $\mathbf{\Phi}\left(t_{j+1}, t_j\right)$ as

$$\mathbf{\Phi}\left(t_{j+1}, t_j\right) = \begin{bmatrix} \mathbf{A}_{j+1,j} & \mathbf{B}_{j+1,j} \\ \mathbf{C}_{j+1,j} & \mathbf{D}_{j+1,j} \end{bmatrix} \tag{30}$$

We can solve for $\Delta\mathbf{v}_j$ such that $\delta\mathbf{r}_{j+1}$ is zero by iterating on Eq. (31) until $(\mathbf{r}_{j+1} - \mathbf{r}_a)$ meets a user defined tolerance.

$$\Delta\mathbf{v}_j = \mathbf{B}_{j+1,j}^{-1}\left(\mathbf{r}_{j+1} - \mathbf{r}_a\right) \tag{31}$$

Upon convergence, for each trajectory arc we save $\mathbf{v}_j^+$, $\mathbf{v}_j^-$, and $\mathbf{\Phi}$ for use in calculating the cost, constraints, and their derivatives. It is important to note that this approach assumes that $\mathbf{B}_{j+1,j}^{-1}$ exists. We address cases when this is not true in a later section. Using the above algorithm, we solve all N Lambert's problems. Knowing the solution to each trajectory arc permits the calculation of all maneuvers Δv_{jk} and with this information we can evaluate J and $\mathbf{G}$.

Step 4: Solve for J and $\mathbf{G}$

From the previous steps we know $\mathbf{v}_{jk}^+$ and $\mathbf{v}_{jk}^-$. We use Eqs. (24) to calculate Δv_{jk}. Next we can evaluate $f_s(\Delta v_{jk})$ using Eqs. (41)-(43). J can be calculated using Eqs. (2) and (3).

The constraints in Eqs. (7) are more conveniently written for mathematical manipulation as

$$\mathbf{G} = \text{diag}\left(\mathbf{Z}\Delta\mathbf{V}\Delta\mathbf{V}^T\mathbf{Z}^T\right) \leq \mathbf{TOL} \tag{32}$$

where $\mathbf{TOL}$ is a vector of tolerances, $\Delta\mathbf{V}$ is given by

$$\Delta\mathbf{V} = \left[\Delta V_1 \;\; \Delta V_2 \;\; \ldots \;\; \Delta V_m\right]^T \tag{33}$$

and $\mathbf{Z}$ is given by

$$\mathbf{Z} = \begin{pmatrix} -1 & 1 & 0 & 0 & \dots & 0 \\ 0 & -1 & 1 & 0 & \dots & 0 \\ 0 & 0 & -1 & 1 & \dots & 0 \\ & & \vdots & & & \\ 0 & \dots & -1 & 1 & 0 & 0 \\ 0 & \dots & 0 & -1 & 1 & 0 \\ 0 & \dots & 0 & 0 & -1 & 1 \\ 1 & 0 & 0 & \dots & 0 & -1 \end{pmatrix}$$

The above equations allow us to calculate $J(\mathbf{X}, \mathbf{C})$, and $\mathbf{G}(\mathbf{X}, \mathbf{C})$. To take full advantage of the power of a numerical optimization routine, it is also useful to calculate the gradient of J and the Jacobian of $\mathbf{G}$. We devote the next section to this topic.

Cost and Constraint Derivatives

Gradient-based numerical optimization routines such as Sequential Quadratic Programming (SQP) perform best when supplied with analytic derivatives of the cost and constraints. Providing derivatives is often nontrivial, yet it is advantageous because it increases the speed of convergence by requiring fewer function calls and avoids numerical problems associated with finite differencing.

Below we derive the gradient of the cost function and the Jacobian of the constraint functions. We need the derivatives of the cost and constraint functions with respect to the independent variables shown in Eqs. (15) and (20). Specifically, we require analytic expressions for

$$\frac{\partial J}{\partial x} = \frac{\partial}{\partial x} \sum_{k=1}^{m} \Delta V_k \tag{34}$$

and

$$\frac{\partial \mathbf{G}}{\partial x} = 2 \text{ diag} \left(\mathbf{Z} \Delta \mathbf{V} \frac{\partial \Delta \mathbf{V}^T}{\partial x} \mathbf{Z}^T \right) \tag{35}$$

where x is a generic independent variable and

$$\frac{\partial \Delta \mathbf{V}}{\partial x} = \left[\frac{\Delta V_1}{\partial x} \quad \frac{\partial \Delta V_2}{\partial x} \quad \dots \quad \frac{\partial \Delta V_m}{\partial x} \right]^T \tag{36}$$

In Eqs. (34)-(36) we see terms of the form $\partial \Delta V_k / \partial x$ which can be written

$$\frac{\partial \Delta V_k}{\partial x} = \frac{\partial}{\partial x} \sum_{j=1}^{n_k} f_s(\Delta v_{jk}) \Delta v_{jk} \tag{37}$$

One can show that Eq. (37) can be written as

$$\frac{\partial \Delta V_k}{\partial x} = \sum_{j=1}^{n_k} \left(\frac{\partial f_s(\Delta v_{jk})}{\partial \Delta v_{jk}} + \frac{f_s(\Delta v_{jk})}{\Delta v_{jk}} \right) \frac{\partial \Delta \mathbf{v}_{jk}^T}{\partial x} \Delta \mathbf{v}_{jk} \tag{38}$$

By inspecting Eq. (38), we see that we must determine $\partial \Delta \mathbf{v}_{jk}^T / \partial x$. This term is non-trivial and in the next few subsections we derive this term for the specific independent variables used in this work. The term $f_s(\Delta v_{jk})/\Delta v_{jk}$ can cause difficulty for small Δv_{jk}. Traditionally, to determine the total ΔV, we would set $f_s = 1$ and we have the new relationship

$$\Delta V_k' = \sum_{j=1}^{n_k} \Delta v_{jk} \tag{39}$$

However, if $f_s = 1$ then we have the following term that appears in the derivative of $\Delta V_k'$:

$$\frac{f_s(\Delta v_{jk})}{\Delta v_{jk}} = \frac{1}{\Delta v_{jk}} \tag{40}$$

This term is obviously singular for small Δv_{jk}. The difficulty this causes is significant because the optimization process tends to make Δv_{jk} as small as possible and sometimes Δv_{jk} can approach zero. We can mitigate problems caused by small values of Δv_{jk} by carefully choosing $f_s(\Delta v_{jk})$.

By inspecting the term $f_s(\Delta v_{jk})/\Delta v_{jk}$, we see that we need $f_s(\Delta v_{jk})$ to approach zero as fast or faster than Δv_{jk} so that the limit as $\Delta v_{jk} \to 0$ is defined. There are many possible choices for such a function. We have chosen to partition the function $f_s(\Delta v_{jk})$ into three regions. For small values of Δv_{jk}, where $\Delta v_{jk} < \Delta v_L$ we define $f_s(\Delta v_{jk})$ as

$$f_s(\Delta v_{jk}) = \Delta v_{jk}^2 \qquad (\Delta v_{jk} < \Delta v_L) \tag{41}$$

For intermediate values of Δv_{jk}, where $\Delta v_L < \Delta v_{jk} < \Delta v_H$, we define $f_s(\Delta v_{jk})$ as

$$f_s(\Delta v_{jk}) = a\Delta v_{jk}^4 + b\Delta v_{jk}^3 + c\Delta v_{jk}^2 + d\Delta v_{jk} \qquad (\Delta v_L < \Delta v < \Delta v_H) \tag{42}$$

For large values of Δv_{jk}, where $\Delta v_H < \Delta v_{jk}$, we define $f_s(\Delta v_{jk})$ as

$$f_s(\Delta v_{jk}) = 1 \quad (\Delta v_H < \Delta v_{jk}) \tag{43}$$

The values of Δv_L and Δv_H in the above equations are chosen depending upon the numerics of the particular problem being solved. However, Δv_L must always be less than Δv_H.

The form of f_s described above removes the singularity in the derivative of $f_s(\Delta v_{jk})$ for small values of Δv_{jk}. As $\Delta v_{jk} \to 0$ we see that where $\Delta v_{jk} < \Delta v_L$

$$\lim_{\Delta v_{jk} \to 0} \frac{f_s(\Delta v_{jk})}{\Delta v_{jk}} = \lim_{\Delta v_{jk} \to 0} \frac{\Delta v_{jk}^2}{\Delta v_{jk}} = 0 \tag{44}$$

and we have a non-singular function for all values of Δv_{jk}. The four constants in the quartic function in Eq. (42) are chosen so that $f_s(\Delta v_{jk})$ and its first derivative are continuous. The derivation of the constants a, b, c, and d is shown in Appendix 1 and the expressions are found in Eqs. (114-117).

The second term in Eq. (38) that is non-trivial is

$$\frac{\partial \Delta \mathbf{v}_{jk}^T}{\partial x} \tag{45}$$

where x is a dummy variable that represents an arbitrary component of $\mathbf{X}$ given in Eqs. (15) and (20). First let's identify some derivatives that are zero after looking at the physics of the problem. From inspection of Figure (1) and (2) we see that

$$\frac{\partial \Delta \mathbf{v}_{jk}^T}{\partial \mathbf{r}_{\ell n}} = \mathbf{0} \text{ if } n \neq k \tag{46}$$

and

$$\frac{\partial \Delta \mathbf{v}_{jk}^T}{\partial t_{in}} = \mathbf{0} \text{ if } n \neq k \tag{47}$$

where n is dummy index used to denote the trajectory number. Eqs. (46) and (47) come from the fact that changing the time or position of a maneuver on one trajectory does not affect the ΔV along another trajectory. For this reason we can drop the subscripts n and k without loss of generality. Hence the remaining derivatives to be calculated are

$$\frac{\partial \Delta \mathbf{v}_j^T}{\partial \mathbf{r}_\ell}, \frac{\partial \Delta \mathbf{v}_j^T}{\partial t_i}$$

where the second subscript on each variable is assumed to be k. For convenience, we break down the derivatives shown above into three categories and devote a subsection to each. The first category contains initial boundary derivatives which are derivatives with respect to t_o, $\mathbf{r}_o$, $\mathbf{v}_o$, and t_1. The second category contains derivatives that are with respect to internal maneuver times and locations, t_ℓ ($t_\ell \in t_i$) and $\mathbf{r}_\ell$ respectively where $2 \leq \ell \leq n_k - 1$. The third category contains derivatives with respect to the final time, t_{n_k}. The next three subsections discuss the three types of derivatives in detail.

Initial Boundary Derivatives

We define the initial boundary derivatives to be those with respect to t_1, t_o, $\mathbf{r}_o$, and $\mathbf{v}_o$. By inspection of Figure (1) we can see that

$$\frac{\partial \Delta \mathbf{v}_j^T}{\partial t_1} = \frac{\partial \Delta \mathbf{v}_j^T}{\partial t_o} = \frac{\partial \Delta \mathbf{v}_j^T}{\partial \mathbf{r}_o} = \frac{\partial \Delta \mathbf{v}_j^T}{\partial \mathbf{v}_o} = \mathbf{0} \text{ if } j > 2 \tag{48}$$

This is due to the fact that changing $\mathbf{r}_0$ does not change $\Delta \mathbf{v}_3$. Likewise changing time t_o does not change $\Delta \mathbf{v}_3$. Therefore the nonzero initial boundary derivatives are

$$\frac{\partial \Delta \mathbf{v}_1^T}{\partial t_1}, \frac{\partial \Delta \mathbf{v}_2^T}{\partial t_1}, \frac{\partial \Delta \mathbf{v}_1^T}{\partial t_o}, \frac{\partial \Delta \mathbf{v}_2^T}{\partial t_o}, \frac{\partial \Delta \mathbf{v}_1^T}{\partial \mathbf{r}_o}, \frac{\partial \Delta \mathbf{v}_2^T}{\partial \mathbf{r}_o}, \frac{\partial \Delta \mathbf{v}_1^T}{\partial \mathbf{v}_o}, \frac{\partial \Delta \mathbf{v}_2^T}{\partial \mathbf{v}_o}$$

Let's begin by looking at the derivatives with respect to t_1. Assume we have the TPBVP illustrated in Figure 4 and defined by

Given: t_o, $\mathbf{r}_o$, $\mathbf{v}_o$, t_1, t_2, $\mathbf{r}_2$
Find: $\mathbf{v}_1^+$ such that $\mathbf{r}\,|_{t_2} = \mathbf{r}_2$

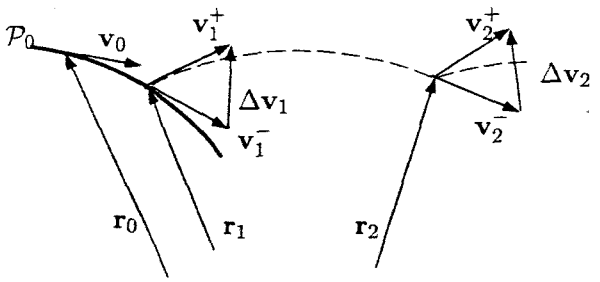

Figure 4 Illustration of Initial Boundary

We know the solution has the following form

$$\mathbf{r}_1 = \phi^r\left(t_1, t_2, \left[\mathbf{r}_2, \mathbf{v}_2^-\right]\right) \tag{49}$$

$$\mathbf{v}_1^+ = \phi^v\left(t_1, t_2, \left[\mathbf{r}_2, \mathbf{v}_2^-\right]\right) \tag{50}$$

The symbol ϕ denotes the solution to the initial value problem with initial conditions contained in square brackets. The second time argument is the initial time and the first time argument is the final time. So, in Eq. (49), $\mathbf{r}_2$ and $\mathbf{v}_2^-$ are the initial conditions with an initial time of t_2 and a final time of t_1. Hence, in this case we are back-propagating because $t_2 > t_1$. The superscript r and v denote the position and velocity portions of the initial value problem respectively. By inspection of Figure 4, we see that changing t_1 will result in a change in $\mathbf{r}_1$, $\mathbf{v}_1^-$, $\mathbf{v}_1^+$, and $\mathbf{v}_2^-$. Taking the derivative of $\mathbf{r}_1$ and $\mathbf{v}_1^+$ with respect to t_1 yields

$$\frac{\partial \mathbf{r}_1}{\partial t_1} = \frac{\partial \phi^r}{\partial t_1} + \frac{\partial \phi^r}{\partial V}\frac{\partial \mathbf{v}_2^-}{\partial t_1} \tag{51}$$

$$\frac{\partial \mathbf{v}_1^+}{\partial t_1} = \frac{\partial \phi^v}{\partial t_1} + \frac{\partial \phi^v}{\partial V}\frac{\partial \mathbf{v}_2^-}{\partial t_1} \tag{52}$$

where V is a dummy variable to denote differentiation with respect to velocity. These equations can be rewritten as

$$\mathbf{v}_1^- = \mathbf{v}_1^+ + \mathbf{B}_{t_1,t_2}\frac{\partial \mathbf{v}_2^-}{\partial t_1} \tag{53}$$

$$\frac{\partial \mathbf{v}_1^+}{\partial t_1} = \mathbf{a}_1^+ + \mathbf{D}_{t_1,t_2}\frac{\partial \mathbf{v}_2^-}{\partial t_1} \tag{54}$$

Solving the system of equations, and using Eqs. (118) and (119) from Appendix 2, we obtain

$$\frac{\partial \mathbf{v}_2^-}{\partial t_1} = \left(\mathbf{C}_{t_2,t_1} - \mathbf{D}_{t_2,t_1}\mathbf{B}_{t_2,t_1}^{-1}\mathbf{A}_{t_2,t_1}\right)\left(\mathbf{v}_1^- - \mathbf{v}_1^+\right) \tag{55}$$

$$\frac{\partial \mathbf{v}_1^+}{\partial t_1} = \mathbf{a}_1^+ - \mathbf{B}_{t_2,t_1}^{-1}\mathbf{A}_{t_2,t_1}\left(\mathbf{v}_1^- - \mathbf{v}_1^+\right) \tag{56}$$

By inspection, we see that

$$\frac{\partial \mathbf{v}_1^-}{\partial t_1} = \mathbf{a}_1^- \tag{57}$$

$$\frac{\partial \mathbf{v}_2^+}{\partial t_1} = 0 \tag{58}$$

The derivatives with respect to $\mathbf{r}_o$ and $\mathbf{v}_o$ can be derived by starting with a solution of the form

$$\mathbf{r}_2 = \phi^r\left(t_2, t_1, [\mathbf{r}_1, \mathbf{v}_1^+]\right) \tag{59}$$

$$\mathbf{v}_2^- = \phi^v\left(t_2, t_1, [\mathbf{r}_1, \mathbf{v}_1^+]\right) \tag{60}$$

where we note that changes in $\mathbf{r}_o$ or $\mathbf{v}_o$ result in changes in $\mathbf{r}_1$, $\mathbf{v}_1^-$, $\mathbf{v}_1^+$, and $\mathbf{v}_2^-$. Taking derivatives of Eqs. (59) and (60) with respect to $\mathbf{r}_o$ yields

$$\frac{\partial \mathbf{r}_2}{\partial \mathbf{r}_o} = \frac{\partial \phi^r}{\partial R}\frac{\partial \mathbf{r}_1}{\partial \mathbf{r}_o} + \frac{\partial \phi^r}{\partial V}\frac{\partial \mathbf{v}_1^+}{\partial \mathbf{r}_o} \tag{61}$$

$$\frac{\partial \mathbf{v}_2^-}{\partial \mathbf{r}_o} = \frac{\partial \phi^v}{\partial R}\frac{\partial \mathbf{r}_1}{\partial \mathbf{r}_o} + \frac{\partial \phi^v}{\partial V}\frac{\partial \mathbf{v}_1^+}{\partial \mathbf{r}_o} \tag{62}$$

where R is dummy variable to denote differentiation with respect to position. These equations can be rewritten as

$$0 = \mathbf{A}_{t_2,t_1}\mathbf{A}_{t_1,t_o} + \mathbf{B}_{t_2,t_1}\frac{\partial \mathbf{v}_1^+}{\partial \mathbf{r}_o} \tag{63}$$

$$\frac{\partial \mathbf{v}_2^-}{\partial \mathbf{r}_o} = \mathbf{C}_{t_2,t_1}\mathbf{A}_{t_1,t_o} + \mathbf{D}_{t_2,t_1}\frac{\partial \mathbf{v}_1^+}{\partial \mathbf{r}_o} \tag{64}$$

Finally, solving for the desired derivatives yields

$$\frac{\partial \mathbf{v}_1^+}{\partial \mathbf{r}_o} = -\mathbf{B}_{t_2,t_1}^{-1}\mathbf{A}_{t_2,t_1}\mathbf{A}_{t_1,t_o} \tag{65}$$

$$\frac{\partial \mathbf{v}_2^-}{\partial \mathbf{r}_o} = \left(\mathbf{C}_{t_2,t_1} - \mathbf{D}_{t_2,t_1}\mathbf{B}_{t_2,t_1}^{-1}\mathbf{A}_{t_2,t_1}\right)\mathbf{A}_{t_1,t_o} \tag{66}$$

Taking derivatives of Eqs. (59) and (60) with respect to $\mathbf{v}_o$ yields

$$\frac{\partial \mathbf{r}_2}{\partial \mathbf{v}_o} = \frac{\partial \phi^r}{\partial R}\frac{\partial \mathbf{r}_1}{\partial \mathbf{v}_o} + \frac{\partial \phi^r}{\partial V}\frac{\partial \mathbf{v}_1^+}{\partial \mathbf{v}_o} \tag{67}$$

$$\frac{\partial \mathbf{v}_2^-}{\partial \mathbf{v}_o} = \frac{\partial \phi^v}{\partial R}\frac{\partial \mathbf{r}_1}{\partial \mathbf{v}_o} + \frac{\partial \phi^v}{\partial V}\frac{\partial \mathbf{v}_1^+}{\partial \mathbf{v}_o} \tag{68}$$

These equations can be rewritten as

$$0 = \mathbf{A}_{t_2,t_1}\mathbf{B}_{t_1,t_o} + \mathbf{B}_{t_2,t_1}\frac{\partial \mathbf{v}_1^+}{\partial \mathbf{r}_o} \tag{69}$$

$$\frac{\partial \mathbf{v}_2^-}{\partial \mathbf{r}_o} = \mathbf{C}_{t_2,t_1}\mathbf{B}_{t_1,t_o} + \mathbf{D}_{t_2,t_1}\frac{\partial \mathbf{v}_1^+}{\partial \mathbf{r}_o} \tag{70}$$

solving for the desired quantities yields

$$\frac{\partial \mathbf{v}_1^+}{\partial \mathbf{v}_o} = -\mathbf{B}_{t_2,t_1}^{-1}\mathbf{A}_{t_2,t_1}\mathbf{B}_{t_1,t_o} \tag{71}$$

$$\frac{\partial \mathbf{v}_2^-}{\partial \mathbf{v}_o} = \left(\mathbf{C}_{t_2,t_1} - \mathbf{D}_{t_2,t_1}\mathbf{B}_{t_2,t_1}^{-1}\mathbf{A}_{t_2,t_1}\right)\mathbf{B}_{t_1,t_o} \tag{72}$$

Finally, the last two nonzero derivatives with respect to $\mathbf{r}_o$ and $\mathbf{v}_o$ can be written simply as

$$\frac{\partial \mathbf{v}_1^-}{\partial \mathbf{r}_o} = \mathbf{C}_{t_1,to} \tag{73}$$

$$\frac{\partial \mathbf{v}_1^-}{\partial \mathbf{v}_o} = \mathbf{D}_{t_1,to} \tag{74}$$

The last initial boundary derivatives to be determined are the derivatives with respect to t_o. The derivatives of $\mathbf{r}_1$ and $\mathbf{v}_1^-$ with respect to t_o can be found by starting with a solution of the form

$$\mathbf{r}_o = \phi^r\left(t_o, t_1, [\mathbf{r}_1, \mathbf{v}_1^-]\right) \tag{75}$$

$$\mathbf{v}_o = \phi^v\left(t_o, t_1, [\mathbf{r}_1, \mathbf{v}_1^-]\right) \tag{76}$$

where we note that changes in t_o result in changes in $\mathbf{r}_1$, $\mathbf{v}_1^-$, $\mathbf{v}_1^+$, and $\mathbf{v}_2^-$. Taking the derivative of Eqs. (75) and (76) with respect to t_o yields

$$\frac{\partial \mathbf{r}_o}{\partial t_o} = \frac{\partial \phi^r}{\partial t_o} + \frac{\partial \phi^r}{\partial R}\frac{\partial \mathbf{r}_1}{\partial t_o} + \frac{\partial \phi^r}{\partial V}\frac{\partial \mathbf{v}_1^-}{\partial t_o} \tag{77}$$

$$\frac{\partial \mathbf{v}_o}{\partial t_o} = \frac{\partial \phi^v}{\partial t_o} + \frac{\partial \phi^v}{\partial R}\frac{\partial \mathbf{r}_1}{\partial t_o} + \frac{\partial \phi^v}{\partial V}\frac{\partial \mathbf{v}_1^-}{\partial t_o} \tag{78}$$

These equations simplify to

$$0 = \mathbf{v}_o + \mathbf{A}_{t_o,t_1}\frac{\partial \mathbf{r}_1}{\partial t_o} + \mathbf{B}_{t_o,t_1}\frac{\partial \mathbf{v}_1^-}{\partial t_o} \tag{79}$$

$$0 = \mathbf{a}_o + \mathbf{C}_{t_o,t_1}\frac{\partial \mathbf{r}_1}{\partial t_o} + \mathbf{D}_{t_o,t_1}\frac{\partial \mathbf{v}_1^-}{\partial t_o} \tag{80}$$

solving for the desired derivatives yields

$$\frac{\partial \mathbf{r}_1}{\partial t_o} = -\left(\mathbf{A}_{t_1,t_o}\mathbf{v}_o + \mathbf{B}_{t_1,t_o}\mathbf{a}_o\right) \tag{81}$$

$$\frac{\partial \mathbf{v}_1^-}{\partial t_o} = -\left(\mathbf{C}_{t_1,t_o}\mathbf{v}_o + \mathbf{D}_{t_1,t_o}\mathbf{a}_o\right) \tag{82}$$

Table 1 Initial Boundary Derivatives with Respect to t_o

Term	∂t_o
$\partial \mathbf{v}_1^-$	$-\mathbf{C}_{t_1,t_o}\mathbf{v}_o - \mathbf{D}_{t_1,t_o}\mathbf{a}_o$
$\partial \mathbf{v}_1^+$	$-\mathbf{D}_{t_1,t_2}(\mathbf{I} - \mathbf{D}_{t_2,t_1}\mathbf{D}_{t_1,t_2})^{-1}\mathbf{C}_{t_2,t_1}(\mathbf{A}_{t_1,t_o}\mathbf{v}_o + \mathbf{B}_{t_1,t_o}\mathbf{a}_o)$
$\partial \mathbf{v}_2^-$	$-(\mathbf{I} - \mathbf{D}_{t_2,t_1}\mathbf{D}_{t_1,t_2})^{-1}\mathbf{C}_{t_2,t_1}(\mathbf{A}_{t_1,t_o}\mathbf{v}_o + \mathbf{B}_{t_1,t_o}\mathbf{a}_o)$
$\partial \mathbf{v}_2^+$	0

Recall that changing t_o changes $\mathbf{r}_1$, $\mathbf{v}_1^-$, $\mathbf{v}_1^+$, and $\mathbf{v}_2^-$. We can find the expressions for $\partial \mathbf{v}_1^+/\partial t_o$ and $\partial \mathbf{v}_2^-/\partial t_o$ starting with solutions of the form

$$\mathbf{v}_1^+ = \boldsymbol{\phi}^v(t_1, t_2, [\mathbf{r}_2, \mathbf{v}_2^-]) \tag{83}$$

$$\mathbf{v}_2^- = \boldsymbol{\phi}^v(t_2, t_1, [\mathbf{r}_1, \mathbf{v}_1^+]) \tag{84}$$

Taking the derivative with respect to t_o yields

$$\frac{\partial \mathbf{v}_1^+}{\partial t_o} = \frac{\partial \boldsymbol{\phi}^v}{\partial R}\frac{\partial \mathbf{r}_2}{\partial t_o} + \frac{\partial \boldsymbol{\phi}^v}{\partial V}\frac{\partial \mathbf{v}_2^-}{\partial t_o} \tag{85}$$

$$\frac{\partial \mathbf{v}_2^-}{\partial t_o} = \frac{\partial \boldsymbol{\phi}^v}{\partial R}\frac{\partial \mathbf{r}_1}{\partial t_o} + \frac{\partial \boldsymbol{\phi}^v}{\partial V}\frac{\partial \mathbf{v}_1^+}{\partial t_o} \tag{86}$$

This can be rewritten as the system of equations below

$$\frac{\partial \mathbf{v}_1^+}{\partial t_o} = \mathbf{D}_{t_1,t_2}\frac{\partial \mathbf{v}_2^-}{\partial t_o} \tag{87}$$

$$\frac{\partial \mathbf{v}_2^-}{\partial t_o} = -\mathbf{C}_{t_2,t_1}(\mathbf{A}_{t_1,t_o}\mathbf{v}_o + \mathbf{B}_{t_1,t_o}\mathbf{a}_o) + \mathbf{D}_{t_2,t_1}\frac{\partial \mathbf{v}_1^+}{\partial t_o} \tag{88}$$

Solving the system of equations for the desired quantities yields

$$\frac{\partial \mathbf{v}_1^+}{\partial t_o} = -\mathbf{D}_{t_1,t_2}(\mathbf{I} - \mathbf{D}_{t_2,t_1}\mathbf{D}_{t_1,t_2})^{-1}\mathbf{C}_{t_2,t_1}(\mathbf{A}_{t_1,t_o}\mathbf{v}_o + \mathbf{B}_{t_1,t_o}\mathbf{a}_o) \tag{89}$$

$$\frac{\partial \mathbf{v}_2^-}{\partial t_o} = -(\mathbf{I} - \mathbf{D}_{t_2,t_1}\mathbf{D}_{t_1,t_2})^{-1}\mathbf{C}_{t_2,t_1}(\mathbf{A}_{t_1,t_o}\mathbf{v}_o + \mathbf{B}_{t_1,t_o}\mathbf{a}_o) \tag{90}$$

Note that Eqs. (89) and (90) contain an element of the inverse of the state transition matrix. See Appendix 2 for a discussion of how this can be calculated without inverting the entire 6 by 6 state transition matrix.

We have completed the derivation of the initial boundary derivatives and they are summarized in Tables 1 - 3. Now we move on to the internal derivatives.

Table 2 Initial Boundary Derivatives with Respect to t_1

Term	∂t_1
$\partial \mathbf{v}_1^-$	$\mathbf{a}_1^-$
$\partial \mathbf{v}_1^+$	$\mathbf{a}_1^+ - \mathbf{B}_{t_2,t_1}^{-1}\mathbf{A}_{t_2,t_1}\left(\mathbf{v}_1^- - \mathbf{v}_1^+\right)$
$\partial \mathbf{v}_2^-$	$\left(\mathbf{C}_{t_2,t_1} - \mathbf{D}_{t_2,t_1}\mathbf{B}_{t_2,t_1}^{-1}\mathbf{A}_{t_2,t_1}\right)\left(\mathbf{v}_1^- - \mathbf{v}_1^+\right)$
$\partial \mathbf{v}_2^+$	0

Table 3 Initial Boundary Derivatives with respect to $\mathbf{r}_o$ and $\mathbf{v}_o$

Term	$\partial \mathbf{r}_o$	$\partial \mathbf{v}_o$
$\partial \mathbf{v}_1^-$	$\mathbf{C}_{t_1,to}$	$\mathbf{D}_{t_1,to}$
$\partial \mathbf{v}_1^+$	$-\mathbf{B}_{t_2,t_1}^{-1}\mathbf{A}_{t_2,t_1}\mathbf{A}_{t_1,t_o}$	$-\mathbf{B}_{t_2,t_1}^{-1}\mathbf{A}_{t_2,t_1}\mathbf{B}_{t_1,t_o}$
$\partial \mathbf{v}_2^-$	$\left(\mathbf{C}_{t_2,t_1} - \mathbf{D}_{t_2,t_1}\mathbf{B}_{t_2,t_1}^{-1}\mathbf{A}_{t_2,t_1}\right)\mathbf{A}_{t_1,t_o}$	$\left(\mathbf{C}_{t_2,t_1} - \mathbf{D}_{t_2,t_1}\mathbf{B}_{t_2,t_1}^{-1}\mathbf{A}_{t_2,t_1}\right)\mathbf{B}_{t_1,t_o}$
$\partial \mathbf{v}_2^+$	0	0

Internal Derivatives

The internal derivatives are defined as derivatives of $\Delta\mathbf{v}_j^T$ with respect to the internal maneuver times and positions, or:

$$\frac{\partial \Delta \mathbf{v}_j^T}{\partial \mathbf{r}_\ell} \quad \begin{cases} 1 \leq & j & \leq n_k \\ 2 \leq & \ell & \leq n_k - 1 \end{cases} \tag{91}$$

and

$$\frac{\partial \Delta \mathbf{v}_j^T}{\partial t_\ell} \quad \begin{cases} 1 \leq & j & \leq n_k \\ 2 \leq & \ell & \leq n_k - 1 \end{cases} \tag{92}$$

By inspection of Figure (1) we can see that some of the derivatives shown in expressions (91) and (92) are zero. For example, changing $\mathbf{r}_3$ does not change $\Delta\mathbf{v}_1$ or $\Delta\mathbf{v}_5$. Likewise we see that changing the time t_3 does not change $\Delta\mathbf{v}_1$ or $\Delta\mathbf{v}_5$. In general we can write

$$\frac{\partial \Delta \mathbf{v}_j^T}{\partial \mathbf{r}_\ell} = \mathbf{0} \text{ if } j < \ell - 1 \text{ or } j > \ell + 1 \tag{93}$$

$$\frac{\partial \Delta \mathbf{v}_j^T}{\partial t_\ell} = \mathbf{0} \text{ if } j < \ell - 1 \text{ or } j > \ell + 1 \tag{94}$$

In other words, changing the time or position of the j^{th} maneuver only changes the following maneuvers: $\Delta\mathbf{v}_{j-1}$, $\Delta\mathbf{v}_j$, and $\Delta\mathbf{v}_{j+1}$. Thus, the only non-zero internal derivatives are

$$\frac{\partial \Delta \mathbf{v}_{\ell-1}^T}{\partial \mathbf{r}_\ell}, \quad \frac{\partial \Delta \mathbf{v}_\ell^T}{\partial \mathbf{r}_\ell}, \quad \frac{\partial \Delta \mathbf{v}_{\ell+1}^T}{\partial \mathbf{r}_\ell}$$

The non-zero internal derivatives can all be determined by closely investigating Lambert's problem. Recall that Lambert's problem is to find $\mathbf{v}_I^+$ and $\mathbf{v}_F^-$, given $\mathbf{r}_I$, t_I, $\mathbf{r}_F$ and t_F. We see that the non-zero internal derivatives can be determined from the derivatives of the solution to Lambert's problem , $\mathbf{v}_I^+$ and $\mathbf{v}_F^-$, with respect to changes in $\mathbf{r}_I$, t_I, $\mathbf{r}_F$ and t_F. These derivatives appear in the literature,[5,7] and they can also be found by the approach

Table 4 Time Derivatives of the Solution to Lambert's Problem

	∂t_I	∂t_F
$\partial \mathbf{v}_I^+$	$\mathbf{a}_I^+ + \mathbf{B}_{t_F,t_I}^{-1}\mathbf{A}_{t_F,t_I}\mathbf{v}_I^+$	$-\mathbf{B}_{t_F,t_I}^{-1}\mathbf{v}_F^-$
$\partial \mathbf{v}_F^-$	$(\mathbf{D}_{t_F,t_I}\mathbf{B}_{t_F,t_I}^{-1}\mathbf{A}_{t_F,t_I} - \mathbf{C}_{t_F,t_I})\mathbf{v}_I^+$	$\mathbf{a}_F^- - \mathbf{D}_{t_F,t_I}\mathbf{B}_{t_F,t_I}^{-1}\mathbf{v}_F^-$

Table 5 Position Derivatives of the Solution to Lambert's Problem

	$\partial \mathbf{r}_I$	$\partial \mathbf{r}_F$
$\partial \mathbf{v}_I^+$	$-\mathbf{B}_{t_F,t_I}^{-1}\mathbf{A}_{t_F,t_I}$	$\mathbf{B}_{t_F,t_I}^{-1}$
$\partial \mathbf{v}_F^-$	$\mathbf{C}_{t_F,t_I} - \mathbf{D}_{t_F,t_I}\mathbf{B}_{t_F,t_I}^{-1}\mathbf{A}_{t_F,t_I}$	$\mathbf{D}_{t_F,t_I}\mathbf{B}_{t_F,t_I}^{-1}$

used in this paper to determine the derivatives of cost and constraints with respect to the independent variables. Table 4 contains a summary of the derivatives of $\mathbf{v}_I^+$ and $\mathbf{v}_F^-$ with respect to changes in the initial and final time t_I and t_F respectively. Table 5 contains a summary of the derivatives of $\mathbf{v}_I^+$ and $\mathbf{v}_F^-$ with respect to changes in the initial and final position $\mathbf{r}_I$ and $\mathbf{r}_F$ respectively. The left hand column of the tables contain the numerator of the derivative definition and the horizontal titles contain the denominator of the derivative definition for a particular derivative. So, for example, we see that

$$\frac{\partial \mathbf{v}_I^+}{\partial t_I} = \mathbf{a}_I^+ + \mathbf{B}_{t_F,t_I}^{-1}\mathbf{A}_{t_F,t_I}\mathbf{v}_I^+ \tag{95}$$

where $\mathbf{B}_{t_F,t_I}^{-1}$ and $\mathbf{A}_{t_F,t_I}$ come from the STM of the trajectory that is the solution to Lambert's problem, $\mathbf{v}_I^+$ is the velocity immediately after the first impulse, and $\mathbf{a}_I^+$ is the acceleration immediately after the first impulse. Using the derivatives in Tables 4 and 5, we can determine the remaining internal derivatives which are summarized in Table 6.

It is interesting to note that the derivatives $\partial \mathbf{v}_\ell^- / \partial t_\ell$ and $\mathbf{v}_\ell^+ / \partial t_\ell$ are explicit functions of the accelerations $\mathbf{a}_\ell^+$ and $\mathbf{a}_\ell^-$. For spacecraft flying in environments with nonconservative forces these terms may be significant. However, when we evaluate Eq. (38), the accelerations appear in pairs such as $(\mathbf{a}_\ell^+ - \mathbf{a}_\ell^-)$. This term is identically zero when the flight regime consists only of conservative forces and so acceleration terms do not come into play unless there are forces that are explicit functions of the spacecraft velocity.

Final Boundary Derivatives

The final boundary derivatives are defined as derivatives of $\Delta \mathbf{v}_j^T$ with respect to t_{n_k}. From inspection, we see that

$$\frac{\partial \Delta \mathbf{v}_j^T}{\partial t_{n_k}} = \mathbf{0} \quad \text{if} \quad j < n-1 \tag{96}$$

Table 6 Interior Derivatives

Term	∂t_ℓ	$\partial \mathbf{r}_\ell$
$\partial \mathbf{v}_{\ell-1}^-$	0	0
$\partial \mathbf{v}_{\ell-1}^+$	$-\mathbf{B}_{t_\ell,t_{\ell-1}}^{-1}\mathbf{v}_\ell^-$	$\mathbf{B}_{t_\ell,t_{\ell-1}}^{-1}$
$\partial \mathbf{v}_\ell^-$	$\mathbf{a}_\ell^- - \mathbf{D}_{t_\ell,t_{\ell-1}}\mathbf{B}_{t_\ell,t_{\ell-1}}^{-1}\mathbf{v}_\ell^-$	$\mathbf{D}_{t_\ell,t_{\ell-1}}\mathbf{B}_{t_\ell,t_{\ell-1}}^{-1}$
$\partial \mathbf{v}_\ell^+$	$\mathbf{a}_\ell^+ + \mathbf{B}_{t_{\ell+1},t_\ell}^{-1}\mathbf{A}_{t_{\ell+1},t_\ell}\mathbf{v}_\ell^+$	$-\mathbf{B}_{t_{\ell+1},t_\ell}^{-1}\mathbf{A}_{t_{\ell+1},t_\ell}$
$\partial \mathbf{v}_{\ell+1}^-$	$(\mathbf{D}_{t_{\ell+1},t_\ell}\mathbf{B}_{t_{\ell+1},t_\ell}^{-1}\mathbf{A}_{t_{\ell+1},t_\ell} - \mathbf{C}_{t_{\ell+1},t_\ell})\mathbf{v}_\ell^+$	$\mathbf{C}_{t_{\ell+1},t_\ell} - \mathbf{D}_{t_{\ell+1},t_\ell}\mathbf{B}_{t_{\ell+1},t_\ell}^{-1}\mathbf{A}_{t_{\ell+1},t_\ell}$
$\partial \mathbf{v}_{\ell+1}^+$	0	0

Table 7 Final Boundary Derivatives with Respect to t_{n_k}

Term	∂t_{n_k}
$\partial \mathbf{v}_{n-1}^-$	0
$\partial \mathbf{v}_{n-1}^+$	$\mathbf{B}_{n_k,n_k-1}^{-1}\left(\mathbf{v}_{n_k}^+ - \mathbf{v}_{n_k}^-\right)$
$\partial \mathbf{v}_n^-$	$\mathbf{a}_{n_k}^- + \mathbf{D}_{n_k,n_k-1}\mathbf{B}_{n_k,n_k-1}^{-1}\left(\mathbf{v}_{n_k}^+ - \mathbf{v}_{n_k}^-\right)$
$\partial \mathbf{v}_n^+$	$\mathbf{a}_{n_k}^+$

Following a similar approach as in the last two sections, the final boundary derivatives are

$$\frac{\partial \mathbf{v}_{n-1}^-}{\partial t_{n_k}} = 0 \tag{97}$$

$$\frac{\partial \mathbf{v}_{n-1}^+}{\partial t_{n_k}} = \mathbf{B}_{n_k,n_k-1}^{-1}\left(\mathbf{v}_{n_k}^+ - \mathbf{v}_{n_k}^-\right) \tag{98}$$

$$\frac{\partial \mathbf{v}_n^+}{\partial t_{n_k}} = \mathbf{a}_{n_k}^+ \tag{99}$$

$$\frac{\partial \mathbf{v}_n^-}{\partial t_{n_k}} = \mathbf{a}_{n_k}^- + \mathbf{D}_{n_k,n_k-1}\mathbf{B}_{n_k,n_k-1}^{-1}\left(\mathbf{v}_{n_k}^+ - \mathbf{v}_{n_k}^-\right) \tag{100}$$

The quantity $\mathbf{v}_{n_k}^+$ is found using

$$\mathbf{v}_{n_k}^+ = \phi^v(t_{n_k}, t_f, [\mathbf{r}_f, \mathbf{v}_f]) \tag{101}$$

and $\mathbf{a}_{n_k}^+$ and $\mathbf{a}_{n_k}^-$ come from Eq. (8) evaluated at the pre and post maneuver conditions for maneuver n_k. The derivatives with respect to t_{n_k} are summarized in Table 7. This completes the derivation of the required derivatives. We now move on to discuss numerical issues and implementation.

Numerical Issues and Implementation

Subtle issues in the implementation of a numerical optimization approach often dramatically influence the speed of convergence and the quality of the solutions. The method presented here has several numerical issues that can be accommodated if they are understood by the analyst. In this section, we address these numerical issues as well as discuss

details of the software implementation of the method used to solve the test cases in the next section. The first difficulty occurs when certain components of the STM are not invertible. The second difficulty is an artifact of the problem parameterization and occurs when the times of two maneuvers are the same. The third difficulty is when there are small ΔVs along a trajectory.

The most obvious numerical difficulty appears in calculating the derivatives of the cost and constraints. The equations for the derivatives in the previous section assume that the components of the STM are invertible. Stern[10] showed three cases in which certain components of the STM are not invertible for the two-body problem. They are:

1. The difference between the initial and final times is an integer multiple of the orbit period.
2. The difference between the initial and final true anomalies is given by $N\pi$, for $N =$ 0,1,2,3, ... (Note that case 1 is a subset of case 2)
3. A certain trigonometric function of the eccentricity and the eccentric anomalies is zero.

The first two cases cause surprisingly less difficulty than one might initially expect. Test cases on the Hohmann transfer, whose solution involves a transfer angle of exactly π, have shown that components of the STM are invertible for transfer angles within 1e-4 degrees of the singularity that occurs at the solution. The result is that the method finds solutions within 1e-6 m/s of the known analytic solution. Furthermore, this method has been developed to solve real-world problems where perturbations are included in the dynamics model. In these cases, the solution rarely occurs exactly at transfer angles $(2N+1)\pi$. Finally, the third case occurs for multiple revolution solutions. The examples investigated in this work did not contain multiple revolution trajectory arcs.

Another subtle singularity arises from the parameterization of the problem. The optimization routine controls the independent variables shown in Eq. (15) for a maintenance or reconfiguration sequence and the independent variables shown in Eq. (20) for an initialization sequence. Suppose we are optimizing a maneuver sequence that contains two spacecraft ($m = 2$) and that each spacecraft performs four maneuvers ($n_1 = n_2 = 4$). For this scenario, t_{22} and t_{32}, the times of the second and third maneuver of the second spacecraft respectively, and $\mathbf{r}_{22}$ and $\mathbf{r}_{32}$, the location of the second and third maneuvers of the second spacecraft respectively, are varied freely by the optimizer. It is possible that during the optimization process, that the optimization routine may try the following:

$$t_{22} = t_{32} \qquad \mathbf{r}_{22} \neq \mathbf{r}_{32} \tag{102}$$

There is no solution to Lambert's problem for the above conditions. Furthermore, as $t_{22} \rightarrow t_{32}$, $\Delta v_{22} \rightarrow \infty$. There are several ways to handle this difficulty. One is to apply a set of constraints such that $t_{ik} - t_{i-1,k} \geq c$ where c is a constant chosen according to the problem being solved. However, if during the optimization process this problem occurs, it is likely that one of the maneuvers is not necessary. The simplest solution is to stop the optimization

process, remove one of the maneuvers, in this case either the maneuver at time t_{22} or t_{32}, and restart the optimization process.

The third numerical difficulty is the singularity that occurs when $f_s(\Delta v_{jk}) = 1$ and $\Delta v_{jk} = 0$ and was discussed in previous sections. By defining $f_s(\Delta v_{jk})$ as in Eq. (41) - (43), we can remove this singularity. Physically, the form chosen for $f_s(\Delta v_{jk})$ removes small values of Δv_{jk} from the cost function. Care must be taken in defining the constants Δv_L and Δv_H according to the problem being solved.

The formulation of the cost function, constraints, and gradients was performed without regard to the specific dynamics model chosen. However, in a software implementation, we must choose a dynamics model including the reference frame in which to express the equations of motion, and the forces and perturbations to include. We have chosen to work in the Earth Mean J2000 Equatorial system. We have chosen to include accelerations from the spherical Earth, J_2, and third body point mass accelerations from the Sun and Moon. The resulting dynamics are given by

$$\ddot{\mathbf{r}}_{21} = -G\frac{(m_2 + m_1)}{r_{21}^3}\mathbf{r}_{21} - \sum_{j=3}^{4} G\left(\frac{m_j}{r_{j1}^3}\mathbf{r}_{j1} - \frac{m_j}{r_{j2}^3}\mathbf{r}_{j2}\right) + \mathbf{a}_{J_2} \tag{103}$$

where a subscript "1" represents the spacecraft, a subscript "2" represents Earth, a subscript "3" represents the sun, a subscript "4" represents the moon, and $\mathbf{r}_{21}$ is the position of the spacecraft with respect to the Earth and so on. The term $\mathbf{a}_{J_2}$ is given by

$$\mathbf{a}_{J_2} = -\frac{3J_2\mu_e R_e}{2r^5}\begin{pmatrix} x - \dfrac{5xz^2}{r^2} \\ y - \dfrac{5yz^2}{r^2} \\ 3z - \dfrac{5z^3}{r^2} \end{pmatrix} \tag{104}$$

where x, y, and z are the inertial components of the spacecraft position vector, and μ_e and R_e are the Earth's gravitational parameter and radius respectively. The STM is calculated by defining

$$\mathbf{x} = \begin{bmatrix} \mathbf{r}^T & \mathbf{v}^T \end{bmatrix}^T \tag{105}$$

then

$$\dot{\mathbf{x}} = \begin{bmatrix} \dot{\mathbf{r}}^T & \dot{\mathbf{v}}^T \end{bmatrix}^T \tag{106}$$

then in first order or state form

$$\mathbf{A} = \frac{\partial \dot{\mathbf{x}}}{\partial \mathbf{x}} \tag{107}$$

The derivatives in Eq. (107), while non-trivial, are well known and not presented here. Finally, the differential equation governing the STM is given by

$$\dot{\mathbf{\Phi}} = \mathbf{A}\mathbf{\Phi} \tag{108}$$

The differential equations shown in Eqs. (103) and (108) are numerically integrated as a coupled system of 42 first-order ordinary differential equations.

The remaining issues involved in the software implementation are concerned with optimizer selection, convergence criteria, scaling, and bookkeeping of the considerable amount of data required to evaluate the cost function and its gradient and the constraint functions and their Jacobian. We have chosen to work in MATLAB and therefore have used the *fmincon* SQP algorithm available in the MATLAB Optimization Toolbox. For speed, all numerical integration of the equations of motion and the STMs is performed by using MATLAB *mex* functions compiled from C code. Likewise, all TPBVPs are solved in mexed C functions. The TolX, TolFun, and TolCon convergence tolerances of *fmincon* were set to 1e-12 for most problems and we refer the reader to the MATLAB Optimization Toolbox[8] documentation for more information on the definition of these settings.

The final issue involves bookkeeping. For each cost function evaluation, we require an initial guess in order to start the TPBVP solver discussed in a previous section. For the first function evaluation, the code uses an initial guess provided by the user. For subsequent cost function evaluations, the code uses solutions from previous cost function evaluations as the initial guess. This assures that the initial guesses for the TPBVPs evolve with the optimizer iterations. There is an STM matrix associated with each segment of each trajectory and these STMs are calculated when the TPBVPs are solved. The STMs for each segment are saved, and then used in the calculation of the Gradient and Jacobian. Great care must be taken to save the STMs in a convenient manner and use them correctly in the equations for the Gradient and Jacobian.

We now move on to discuss several example applications.

Applications and Examples

In recent years, numerous distributed spacecraft missions have been proposed in a diverse set of flight regimes and employing a wide range of inter-spacecraft separation distances. The examples we have chosen demonstrate the applicability of the method to different flight regimes and different types of distributed spacecraft missions. In example 1, case 1, we choose not to solve for the optimal injection orbit. In example 1, case 2, we do solve for the optimal injection orbit. Similarly, in some cases we have chosen to apply the $\Delta\mathbf{V}$ equalization constraints, and in other cases we have chosen not to apply the constraints.

The first example is a Highly Elliptic Orbit (HEO) formation of four spacecraft that forms an ideal tetrahedron with sides of 100 km at apogee. For this HEO formation, we apply the method to initialize the tetrahedron in the presence of perturbations for three cases:

1. Minimize J, do not vary injection orbit, do not apply $\Delta\mathbf{V}$ equalization constraints.
2. Minimize J, vary the injection orbit, do not apply $\Delta\mathbf{V}$ equalization constraints.
3. Minimize J, vary the injection orbit, apply $\Delta\mathbf{V}$ equalization constraints.

The second example is a formation in a large-amplitude Lissajous orbit about the Sun-Earth L_2 point. The formation is composed of two spacecraft that initially have the same

state and epoch. The final configuration is a separation of 200 km between the two spacecraft. For this example, we present an optimal initialization sequence to demonstrate the applicability of the method to multi-body flight regimes.

Example 1: HEO Formation

Recall that example 1 is a HEO formation of four spacecraft that forms an ideal tetrahedron of 100 km at apogee. The desired final orbit states are found in Table 8. The initial orbit, called the injection orbit, is found in column five. The desired final states for the spacecraft are found in columns one through four. The injection orbit was determined by back-propagating the desired final states for approximately 24 hours, and averaging the states of the four spacecraft. A three maneuver initial guess sequence was then created by solving the resulting four lambert problems and adding a small intermediate ΔV for a total of three maneuvers on each of the four trajectories. The ΔVs for the initial guess found using this approach are shown in Table (9). We see that the total ΔV for the initial guess is 256.63 m/s.

Table 8 States Defining Desired Orbit for Example 1

Property	S/C 1†	S/C 2†	S/C 3†	S/C 4†	Injection Orbit‡
a (km)	42095.74	42095.74	42095.74	42095.74	42095.70
e	.8181803	.8181822	.8162243	0.8169300	0.8173807
i $(deg.)$	18.00000	18.00000	18.02006	17.94851	17.99215
ω $(deg.)$	90.00012	90.09161	90.04603	90.04597	90.04581
Ω $(deg.)$	0.1020429e-3	0.1026448e-3	.1024955e-3	0.1023461e-3	0
ν $(deg.)$	178.6875	178.6709	178.6699	178.6733	179.9916

‡ 22 Mar 2012 12:00:00.0000 † 23 Mar 2012 11:17:34.2939

Table 9 ΔV's for Initial Guess for Example1, Case One

Property	S/C 1	S/C 2	S/C 3	S/C 4
Δv_1 (m/s)	24.78	21.87	33.98	35.01
Δv_2 (m/s)	6.97	7.058	5.964	6.357
Δv_3 (m/s)	20.04	22.44	36.87	35.28
$\sum \Delta v_j$ (m/s)	51.79	51.37	76.82	76.65

Total $\Delta V = 256.63$ m/s

For example 1, case 1, an optimal maneuver sequence was found for the HEO formation by selecting the independent variables $\mathbf{X}$ and the constants $\mathbf{C}$ as shown in equations Eqs. (15) and (16). Hence, we treated this as a reconfiguration problem where initially the spacecraft were collocated at the same point on the initial orbit. We did not vary the state of the initial orbit, and we did not apply the $\Delta\mathbf{V}$ equalization constraints. The ΔVs associated with the optimal solution for case 1 are found in Table 10. We see the total ΔV is 71.476 m/s and maximum accumulated ΔV for a single spacecraft is about 20 m/s. This is a fuel savings of 185 m/s over the initial guess.

Table 10 Optimal Solution: Example 1, Case 1

Property	S/C 1	S/C 2	S/C 3	S/C 4
Δv_1 (m/s)	8.864	8.783	5.372	6.593
Δv_2 (m/s)	1.475	2.258	3.276	6.33
Δv_3 (m/s)	5.797	6.438	8.899	7.572
$\sum \Delta v_j$ (m/s)	15.956	17.479	17.5466	20.495

Total $\Delta V = 71.476$ m/s

For case 2, we began with the converged solution to case 1 as the initial guess, but allowed the initial orbit to be included in the independent variables as opposed to being considered a constant. Hence, $\mathbf{X}$ and $\mathbf{C}$ were defined as shown in equations Eqs. (20) and (21). The solution yields a minimum fuel maneuver sequence, and the optimal launch injection orbit. The ΔVs for case 2 are shown in Table 11 and the optimal launch injection orbit in Table 12. The total ΔV for case 2 is 20.79 m/s. We see that varying the injection orbit has a dramatic influence on the total ΔV. There is a 51 m/s improvement over case 1 and the maximum accumulated ΔV for a single spacecraft is about 7.3 m/s.

Table 11 Optimal Solution: Example 1, Case 2

Property	S/C 1	S/C 2	S/C 3	S/C 4
Δv_1 (m/s)	0.247	4.187	1.003	4.5e-5
Δv_2 (m/s)	0.523	0.593	2.382	7.212
Δv_3 (m/s)	3.836	4.1e-5	0.791	3.6e-5
$\sum \Delta v_j$ (m/s)	4.606	4.780	4.176	7.212

Total $\Delta V = 20.774$ m/s

Table 12 Example 1, Case 2 Optimal Injection Orbit

Property	Injection Orbit†
a (km)	42091.69
e	0.8168908
i (deg.)	17.999768
ω (deg.)	89.78643
Ω (deg.)	0.181559
ν (deg.)	180.14348

† 22 Mar 2012 11:58:35.4160

For case 3, we choose the same independent variables as example two, however we applied the ΔVequalization constraints shown in Eq. (32). We used the solution from Example 1, case 2 as the initial guess for case 3. The ΔVs for an optimal solution for case 3 are shown in Table 13. Notice that the total $\Delta V$for each spacecraft is 6.093 m/s. Comparing to case 2 we see that enforcing the ΔVequalization constraints resulted in a small penalty of about 3.34 m/s. We now move on to discuss Example 2.

Table 13 Optimal Solution: Example 1, Case 3

Property	S/C 1	S/C 2	S/C 3	S/C 4
Δv_1 (m/s)	0.789	5.151	1.460	0.002
Δv_2 (m/s)	2.460	1.940	3.254	6.068
Δv_3 (m/s)	2.844	0.002	1.379	0.023
$\sum \Delta v_j$ (m/s)	6.093	6.093	6.093	6.029

Total $\Delta V = 24.116$ m/s

Example 2: Libration Point Formation

The second example consists of a two-spacecraft libration point formation problem about the Sun-Earth L_2 point. The desired states of the spacecraft after the maneuver sequence, and the injection orbit and initial epoch are shown in Table 14. The states are for a large-amplitude Lissajous orbit. The initial guess maneuver sequence for Example 2 contains

Table 14 States Defining Desired Orbit for Example 2

Property	S/C 1†	S/C 2†	Injection Orbit‡
x (km)	76863.56215	76915.15497	-70150.29946
y (km)	-407755.1147	-407729.4652	1358773.158
z (km)	-33798.44889	-33989.96985	983153.4317
$\dot{x}$ (km/s)	-0.04802618	-0.048026184	-0.10552622
$\dot{y}$ (km/s)	1.12799544	1.127995438	-0.00980635
$\dot{z}$ (km/s)	0.13812967	0.138129667	-0.05853318

† 11-Jan-2004 09:35:33.6099 ‡ 09-Jul-2004 09:35:33.6099

four maneuvers for each of the two spacecraft. The two internal maneuvers were computed by first finding a two-maneuver trajectory and then placing two small maneuvers, spaced equally in time, along the original two-maneuver trajectory. The ΔVs associated with the initial guess for Example 2 are found in Table 15. The total ΔV for the initial guess for each spacecraft is about 2.6 m/s.

We chose to treat this problem as a formation maintenance problem and we did not vary the initial orbit. Furthermore, due to the fact that the ΔV of the initial guess is already small, we did not apply the ΔV equalization constraints.

The ΔVs for the optimal maneuver sequence for Example 2 are shown in Table 16. Comparing the optimal solution to the initial guess we see that the optimal solution is about a one order-of-magnitude improvement over the initial guess. Also, while we did not enforce the ΔV equalization constraints, the ΔVs for the optimal solution are nearly equal at approximately 0.109 m/s.

Table 15 ΔVs for Initial Guess for Test Case Two

Property	S/C 1	S/C 2
Δv_1 (m/s)	0.2272	0.2272
Δv_2 (m/s)	1.171	1.171
Δv_3 (m/s)	1.098	1.087
Δv_4 (m/s)	0.1766	0.28
$\sum \Delta v_j$ (m/s)	2.6728	2.7651

Total $\Delta V = 5.4379$ m/s

Table 16 Optimal Solution: Example 2

Property	S/C 1	S/C 2
Δv_1 (m/s)	0.05679	0.0568
Δv_2 (m/s)	0.04973	0.04972
Δv_3 (m/s)	4.058e-005	4.066e-005
Δv_4 (m/s)	0.00279	.00275
$\sum \Delta v_j$ (m/s)	0.10935	0.10932

Total $\Delta V = 0.21867$ m/s

Conclusions

Distributed spacecraft and formation flying missions have been proposed for numerous flight regimes and for a wide range of interspacecraft separations. It is useful for the mission analyst to have at his or her disposal a method that is applicable to as many mission scenarios and dynamics regimes as possible to perform optimal maneuver planning.

In this work we presented a direct approach to find minimum fuel maneuver sequences for distributed spacecraft missions. The cost function is defined as the cumulative ΔV of all spacecraft in formation and we proposed a set of optional constraints to equalize the fuel expenditure among spacecraft over a particular maneuver sequence. The method requires solving a set of IVPs and TPBVPs for each cost function evaluation. However, given the speed of modern computers the method is not prohibitively slow. Analytic derivatives of the cost and constraints were derived to take full advantage of the power of the numerical optimization routine. The method was applied to two test problems: a HEO formation and a libration point formation. Several optimal scenarios were presented.

Their are several new contributions to the literature contained in this work. We generalized methods previously developed in Refs [3] - [7], to permit minimum fuel optimization for a set of m spacecraft. We also generalized the method to find the optimal launch vehicle injection orbit to minimize fuel during the initial spacecraft deployment phase. The cost function was reformulated to remove a naturally occurring singularity in the gradient, without loss of generality. We also formulated a set of constraints to equalize the fuel expenditure among spacecraft. These modifications, together with the work performed by previous researchers, provides an optimization technique for minimum fuel distributed

spacecraft maneuvers in multiple flight regimes including LEO, HEO, libration and interplanetary trajectories. Furthermore, the method is not limited to small interspaceraft separations and is applicable to small formations or large constellations.

REFERENCES

1. J. Betts, "Survey of Numerical Methods for Trajectory Optimization," *Journal of Guidance, Control and Dynamics*, Vol. 21, March-April 1998, pp. 193–207.

2. J. Guzmán, L. Mailhe, C. Schiff, S. Hughes, and D. Folta, "Primer Vector Optimization: Survey of Theory, New Analysis and Applications," *53rd International Astronautical Congress*, Houston, Texas, October 2002. IAC-02-A.6.09.

3. W.H. Goodyear, "A General Method for the Computation of Cartesian Coordinates and Partial Derivatives of the Two-Body Problem," *NASA Report CR-522*, Sept. 1966.

4. S. Bayliss, "Precision Targeting for Multiple Swingby Interplanetary Trajectories," *AIAA 9th Aerospace Sciences Meeting*, New York, New York, Jan. 25-27, 1971.

5. L. A. D'Amario, D. V. Byrnes, L. L. Sackett, and R. H. Stanford, "Optimization of Multiple Flyby Trajectories," *AAS/AIAA Astrodynamics Conference*, Provincetown, Massachusetts, June. 1979.

6. K. C. Howell and H. J. Pernicka, "Numerical Determination of Lissajous Trajectories in The Restricted Three-Body Problem," *Celestial Mechanics*, Vol. 41, 1988, pp. 107–124.

7. R. S. Wilson and K. C. Howell, "A Design Concept for Multiple Lunar Swingby Trajectories," *AIAA/AAS Astrodynamics Conference*, Scottsdale, AZ, Aug. 1994.

8. The MathWorks, "Optimization Toolbox Documentation," *http://www.mathworks.com.*

9. K. R. Meyer and G. R. Hall, *Introduction to Hamiltonian Dynamical Systems and the N-Body Problem.* Springer-Verlag, New York, 1992.

10. R. G. Stern, "Singularities in The Analytic Solution of the Linearized Variational Equations of Elliptical Motion," *AIAA Journal*, July, 1 1964, pp. 1–13.

Appendix 1

In Table 17, we see the three forms that the function $f_s(\Delta v_{jk})$ can assume depending on the magnitude of Δv_{jk}. The constants in the quartic equation are chosen so that f_s and its first derivative are continuous for all values of Δv_{jk}. If we label the different portions of f_s as F_1, F_2, and F_3 as shown in Figure 5, then the conditions to ensure a continuous function and its first derivative are

$$\left.\frac{\partial F_1}{\partial \Delta v}\right|_{\Delta v_L} = \left.\frac{\partial F_2}{\partial \Delta v}\right|_{\Delta v_L} \tag{109}$$

Table 17 Definition of $f_s(\Delta v_{jk})$ for different values of Δv_{jk}

Δv_{jk}	$f_s(\Delta v_{jk})$
$\Delta v_{jk} < \Delta v_L$	Δv_{jk}^2
$\Delta v_L < \Delta v_{jk} < \Delta v_H$	$a\Delta v_{jk}^4 + b\Delta v_{jk}^3 + c\Delta v_{jk}^2 + d\Delta v_{jk}$
$\Delta v_H < \Delta v_{jk}$	1

$$F_1(\Delta v_L) = F_2(\Delta v_L) \tag{110}$$

$$\left.\frac{\partial F_2}{\partial \Delta v}\right|_{\Delta v_H} = 0 \tag{111}$$

$$F_2(\Delta v_H) = 1 \tag{112}$$

These conditions yield the following system of linear, algebraic equations

$$\begin{pmatrix} 4\Delta v_L^3 & 3\Delta v_L^2 & 2\Delta v_L & 1 \\ \Delta v_L^4 & \Delta v_L^3 & \Delta v_L^2 & \Delta v_L \\ 4\Delta v_H^3 & 3\Delta v_H^2 & 2\Delta v_H & 1 \\ \Delta v_H^4 & \Delta v_H^3 & \Delta v_H^2 & \Delta v_H \end{pmatrix} \begin{pmatrix} a \\ b \\ c \\ d \end{pmatrix} = \begin{pmatrix} 2\Delta v_L \\ \Delta v_L^2 \\ 0 \\ 1 \end{pmatrix} \tag{113}$$

The solution to this system of equations is

$$a = -\frac{\Delta v_L \Delta v_H^2 + \Delta v_L + \Delta v_H^3 - 3\Delta v_H}{(-\Delta v_H + \Delta v_L)^3 \Delta v_H^2} \tag{114}$$

$$b = 2\frac{\Delta v_L^2 \Delta v_H^2 + \Delta v_L^2 + \Delta v_H^3 \Delta v_L - 2\Delta v_L \Delta v_H + \Delta v_H^4 - 2\Delta v_H^2}{(-\Delta v_H + \Delta v_L)^3 \Delta v_H^2} \tag{115}$$

$$c = -\frac{\Delta v_L^3 + \Delta v_L^2 \Delta v_H + 4\Delta v_H^3 \Delta v_L^2 + \Delta v_H^4 \Delta v_L - 8\Delta v_L \Delta v_H^2 + \Delta v_H^5}{(-\Delta v_H + \Delta v_L)^3 \Delta v_H^2} \tag{116}$$

$$d = 2\frac{(\Delta v_L + \Delta v_H^3 - 2\Delta v_H)\Delta v_L^2}{\Delta v_H (-\Delta v_H + \Delta v_L)^3} \tag{117}$$

Appendix 2

In order to calculate all of the required partial derivatives, it is sometimes necessary to calculate the inverse of the state transition matrix. Using well known formulas for the inverse of a block matrix, and assuming that all of the necessary inverses exist, one can show that

$$\boldsymbol{\Phi}(t_{j+1}, t_j)^{-1} = \begin{bmatrix} \boldsymbol{A}_{j+1,j} & \boldsymbol{B}_{j+1,j} \\ \boldsymbol{C}_{j+1,j} & \boldsymbol{D}_{j+1,j} \end{bmatrix}^{-1} =$$
$$\begin{bmatrix} (\boldsymbol{A}_{j+1,j} - \boldsymbol{B}_{j+1,j}\boldsymbol{D}_{j+1,j}^{-1}\boldsymbol{C}_{j+1,j})^{-1} & (\boldsymbol{C}_{j+1,j} - \boldsymbol{D}_{j+1,j}\boldsymbol{B}_{j+1,j}^{-1}\boldsymbol{A}_{j+1,j})^{-1} \\ (\boldsymbol{B}_{j+1,j} - \boldsymbol{A}_{j+1,j}\boldsymbol{C}_{j+1,j}^{-1}\boldsymbol{D}_{j+1,j})^{-1} & (\boldsymbol{D}_{j+1,j} - \boldsymbol{C}_{j+1,j}\boldsymbol{A}_{j+1,j}^{-1}\boldsymbol{B}_{j+1,j})^{-1} \end{bmatrix}$$

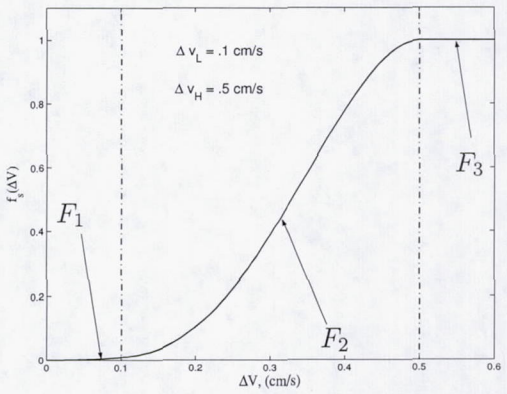

Figure 5 Illustration of $f_s(\Delta V)$

From the above, we determine that

$$\boldsymbol{B}_{j,j+1}^{-1} = \boldsymbol{C}_{j+1,j} - \boldsymbol{D}_{j+1,j}\boldsymbol{B}_{j+1,j}^{-1}\boldsymbol{A}_{j+1,j} \tag{118}$$

$$\boldsymbol{D}_{j,j+1}\boldsymbol{B}_{j,j+1}^{-1} = -\boldsymbol{B}_{j+1,j}^{-1}\boldsymbol{A}_{j+1,j} \tag{119}$$

The relations above can be useful in reconciling the various expressions for the partial derivatives found in the literature. It should also be noted that for Hamiltonian systems, the state transition matrix is *symplectic*[9] which implies that

$$\boldsymbol{\Phi}(t_{j+1},t_j)^{-1} = \begin{bmatrix} \boldsymbol{A}_{j+1,j} & \boldsymbol{B}_{j+1,j} \\ \boldsymbol{C}_{j+1,j} & \boldsymbol{D}_{j+1,j} \end{bmatrix}^{-1} = \begin{bmatrix} \boldsymbol{D}_{j+1,j}^T & -\boldsymbol{B}_{j+1,j}^T \\ -\boldsymbol{C}_{j+1,j}^T & \boldsymbol{A}_{j+1,j}^T \end{bmatrix}$$

Appendix 3: Notation

$\mathbf{r}$	Position vector
$\mathbf{v}$	Velocity vector
m	Number of spacecraft in formation
n_k	Number of maneuvers along k^{th} trajectory
$\mathbf{\Phi}$	State transition matrix
$\mathbf{A}$	Upper left 3x3 partition of $\mathbf{\Phi}$
$\mathbf{B}$	Upper right 3x3 partition of $\mathbf{\Phi}$
$\mathbf{C}$	Lower left 3x3 partition of $\mathbf{\Phi}$
$\mathbf{D}$	Lower right 3x3 partition of $\mathbf{\Phi}$
$\Delta\mathbf{v}_{jk}$	j^{th} impulsive maneuver on k^{th} trajectory
Δv_{jk}	Magnitude of j^{th} maneuver on k^{th} trajectory
$\mathcal{P}_{ok}$	Initial trajectory of k^{th} spacecraft
$\mathcal{P}_{fk}$	Final trajectory of k^{th} spacecraft
$\mathbf{X}$	Vector of independent variables
$\mathbf{C}$	Vector of constants
i	Internal maneuver location index, $2 \leq i \leq n_k - 1$
j	Maneuver time index, $1 \leq j \leq n_k$
k	Trajectory index, $1 \leq k \leq m$